

Transition State for Aggregation and Reorganization of Normal Fatty Alcohols at the Air/Water Interface

Yu. B. Vysotsky,[†] V. S. Bryantsev,[†] V. B. Fainerman,[‡] D. Vollhardt,^{*,§} R. Miller,[§] and E. V. Aksenenko^{||}

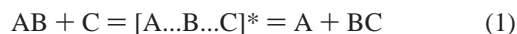
Donbas Academy of Civil Engineering and Architecture, 2 Derzavina Str., Makijivka 86123, Ukraine, Medical Physicochemical Center, Donetsk Medical University, 16 Ilych Avenue, Donetsk 83003, Ukraine, Max Planck Institute of Colloids and Interfaces, 14424 Potsdam/Golm, Germany, and Institute of Colloid Chemistry and Chemistry of Water, 42 Vernadsky Avenue, 03680 Kyiv (Kiev), Ukraine

Received: July 18, 2003; In Final Form: November 6, 2003

The transition state between the initial and final clustering products is analyzed with special reference to the two-dimensional cluster formation and reclustering in the monolayers of normal fatty alcohols ($n = 8-16$). The calculations were performed using the PM3 molecular orbital approximation implemented in the Mopac 2000 software. It is shown that taking into account the enthalpy factor only does not lead to any saddle point at the potential energy surface. This point is reproduced if the entropy factor is assumed. A linear dependence of enthalpy, entropy, and Gibbs free energy on the number of the carbon atoms n is shown to exist for any positions of the system at the reaction coordinate, including the positions of the transition state. This fact was used to construct an additive scheme for the description of transition states in clustering and reclustering reactions in fatty alcohol monolayers for any arbitrary size of the initial cluster. It is shown that in the kinetic formalism the formation of linear clusters is more probable as compared with the formation of star clusters, whereas the attachment of any linear cluster to a star cluster is preferential both from the kinetic and thermodynamic considerations. The dependence of the parameters of the activated complex, corresponding to the dimerization reaction of n -alcohols, on alkyl chain length and temperature is analyzed. The results of the theoretical calculations are in qualitative agreement with experimental data obtained for tetradecanol monolayers.

Introduction

The theory of the elementary unit process of a chemical reaction is based on the transition state concept.¹⁻³ For the chemical reaction in which molecule AB reacts with atom C to form the A and BC entities, the elementary process should pass the saddle point at the potential energy surface, corresponding to the transition state for the reaction considered. In this context, the transition state structure is located between the initial and final states:



There is a lack of any rigorous quantum mechanical theory for the absolute reaction rate. However, the quantum chemical methods are the only source of information about the structure of the transition state. Moreover, one of the principal goals of the quantum chemical analysis is to construct the potential energy (sub)surface and to localize the stationary points that correspond to energy minima and transition states. For ordinary chemical reactions, there exist efficient calculation algorithms⁴⁻⁶ that could be applied to search for the transition state.

For the isothermal–isobaric conditions, the kinetics of the formation of a new phase is determined by the Gibbs energy of the new phase formation ΔG and the viscous flow activation

energy Q as $J = k \exp[-(\Delta G + Q)/RT]$, where J is the new phase formation rate and k is the constant.⁷ For the equilibrium nucleus of a new phase the chemical potential in the initial and emerging phases could be assumed equal to each other; thus the ΔG value for the nucleus of critical size (with zero derivative of ΔG with respect to the radius) can be expressed via the interface tension γ (for the three-dimensional nuclei) or linear tension κ (for two-dimensional nuclei). Neglecting the variation in the chemical potential of the initial phase, one obtains $\Delta G = \gamma A/3$ or $\Delta G = \kappa L/2$, respectively;⁷ here A is the surface area of the three-dimensional nucleus, and L is the perimeter of the two-dimensional nucleus. However, this description is irrelevant in the case of the formation of small two-dimensional clusters, because the nucleus can either exist in the nonequilibrium state or possess noncritical size, and also because the L and κ values for the entities of molecular size are indefinite. We believe that the most relevant approach to the description of growth and reorganization kinetics for molecular clusters the quantum chemical methods which provide the ΔG value directly are the most appropriate. To the best of our knowledge, no quantum chemical studies of phase transition kinetics were performed so far, whereas the cluster formation and reorganization reactions also can be described by eq 1, with A , B , and C (which in physico-organic chemistry stand for atoms or groups of atoms) representing the molecules or groups of molecules which form the cluster. In the present work, the attempt is made to extend the formalism of the transition state theory onto supramolecular chemical systems. As an illustration we consider the geometrical and thermodynamic characteristics of the transition states for

* Corresponding author.

[†] Donbas Academy of Civil Engineering and Architecture.

[‡] Donetsk Medical University.

[§] Max Planck Institute of Colloids and Interfaces.

^{||} Institute of Colloid Chemistry and Chemistry of Water.

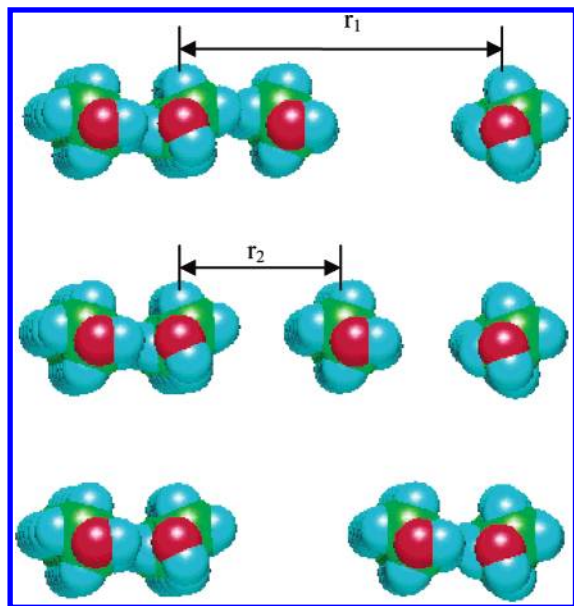


Figure 1. Reaction of the reorganization of trimer and monomer into two dimers (schematically). For the translation motion the reaction coordinates are r_1 and r_2 .

growth and reorganization of two-dimensional clusters of fatty alcohols with the general composition $C_nH_{2n+1}OH$ at the air/water interface. The ground-state parameters for these systems have been studied earlier.^{8,9}

Methods

Calculations were performed using the PM3 molecular orbital approximation, which was included in the Mopac 2000 software¹⁰ run on an IBM PC. According to the statistical mechanical approach, the entropy of a system can be represented as the sum of translation, rotation, and vibration constituents. Assuming that no free rotation takes place in the system, one can express the rotation and translation entropy constituents at any point via the molecular mass, moments of inertia (e.g., the molecular geometry), and temperature, see, e.g., ref 11. The vibration contribution is more difficult to calculate. Usually, the harmonic approximation is most common; i.e., only the first- and second-order terms in the expansion of the energy $E(r)$ into the Taylor series in the vicinity of the stationary point with

respect to the coordinate r are taken into account:

$$E(r) \approx E(r_0) + \frac{dE}{dr}(r - r_0) + \frac{1}{2} \frac{d^2E}{dr^2}(r - r_0)^2 \quad (2)$$

As the first derivative is zero in the stationary point, the calculation of the vibration spectrum requires the diagonalization of the force constants matrix (the second derivatives of the energy with respect to coordinates). It should be stressed that, whereas the matrix of force constants could be defined for any particular geometry (also for the points which do not correspond to any minimum at the potential energy (hyper)surface), the diagonalization of this matrix, i.e., the transformation to normal coordinates, is physically reasonable at the stationary points only. In any other case, to determine the set of vibration natural frequencies, one should first eliminate the projections onto the gradient direction from the force constants matrix¹¹ (e.g., using the projection technique). This procedure was not implemented in MOPAC and other software packages, and therefore, for the calculation of entropy in the nonstationary points the imaginary vibration frequencies should be disregarded, similarly to the calculation of ΔS in the points where the potential energy is maximal. Note also that, even in the stationary points, the vibration frequencies are calculated with quite significant errors in the range of +50 to $i50 \text{ cm}^{-1}$ ¹⁰ due to the fact that the numerical differentiation is used. At the same time, these are the low-frequency vibrations that are characteristic of the molecular clusters and were observed in the experiments.^{13,14} Therefore, the results of the calculations discussed below should be regarded as an initial estimate.

Results and Discussion

Consider the reorganization of a linear trimer and monomer of decanol into two dimers (see Figure 1); this case is the simplest one from the quantum chemical viewpoint, because both breaking and forming $H \cdots H$ bonds are of the same type; cf. ref 9. Here the reaction coordinates are the distance r_1 between the dimer A and monomer C and the distance r_2 between the dimer A and monomer B. For the sake of simplicity we assume the translational motion of the B monomer from A to C. The potential energy sections for different values of the reaction coordinate r_1 are shown in Figure 2; here the minima correspond to the initial and final state shown in Figure 1. It is

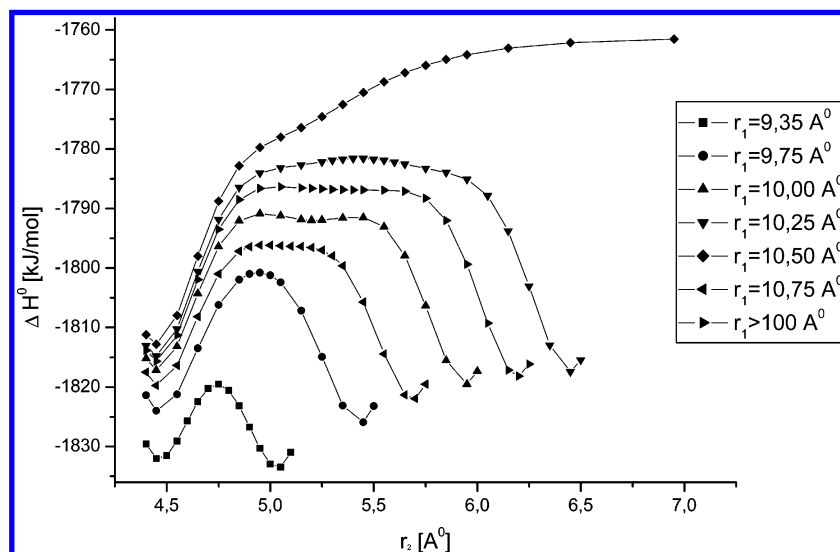


Figure 2. Potential energy profile for translational movement of the n -tetradecanol molecule from dimer to monomer.

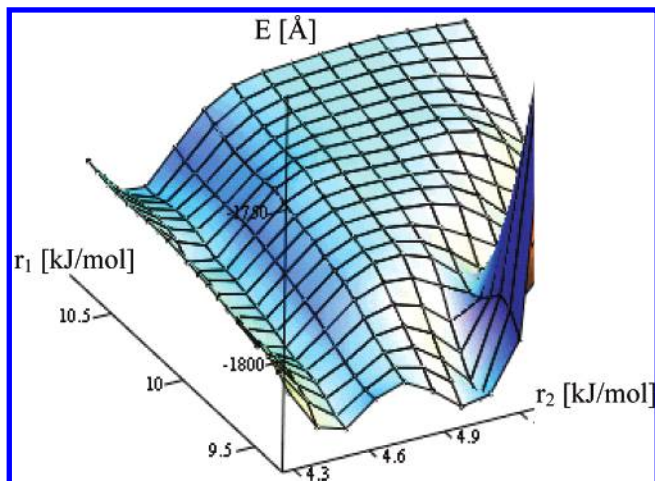


Figure 3. Potential energy surface for translational movement of the *n*-tetradecanol molecule from dimer to monomer.

seen that, for any fixed r_1 value there exists a potential barrier; however, this cannot be regarded as the evidence that the transition state exists.

The potential surface of the analyzed reaction is shown in Figure 3. It is seen that the left valley corresponds to the initial entities (trimer and monomer), whereas the right valley represents the expected reaction products. The heights of the valleys and of the crest, which separates the valleys, become monotonically lower with the decrease of r_1 value. At $r_1 = 4.45$ Å these valleys are seen to intersect each other, which corresponds to the global minimum at this potential (hyper)surface, i.e., the formation of tetramer. For the saddle point at the potential energy (hyper)surface to exist, it is necessary for the sign of the second derivative of energy to be dependent on the direction along which this derivative is calculated.

As no minimum exists along any direction, and the potential barriers in Figure 2 become lower with the decrease of r_1 , the potential energy (hyper)surface does not exhibit any saddle point. Therefore, the reactions shown in Figure 1 cannot take place, and the system should "slither" toward the global minimum that corresponds to the tetramer formation (no activation energy). This is why the standard routines, used by MOPAC and other quantum chemical software packages¹⁰ to search for the transition state, fail to converge in this point, and the resulting configuration of the system corresponds to the joint cluster. As this search was not constrained to the translational motion along the reaction coordinate only, this result is of general character.

In terms of rigorous analysis, this is the Gibbs energy, not the enthalpy, which determines the possibility of a spontaneous reaction:

$$\Delta G = \Delta H - T\Delta S \quad (3)$$

Therefore, in addition to the enthalpy, the entropy constituent should be considered. For the process shown in Figure 1, the maximum points on the curves in Figure 2 for low r_1 values correspond to the limit of one entity. At the same time, for $r_1 \rightarrow \infty$ three entities exist; therefore the entropy of the system becomes higher with the increase of r_1 . As both the enthalpy and the entropy of the cluster (cf. Figures 4 and 5) become higher in these points with the increase of r_1 value (leading therefore to the decrease of the $-T\Delta S$ value), then one should expect the extremal behavior of the dependence of the Gibbs energy on r_1 . This extremum could be either minimum or maximum; therefore, it becomes necessary to calculate the

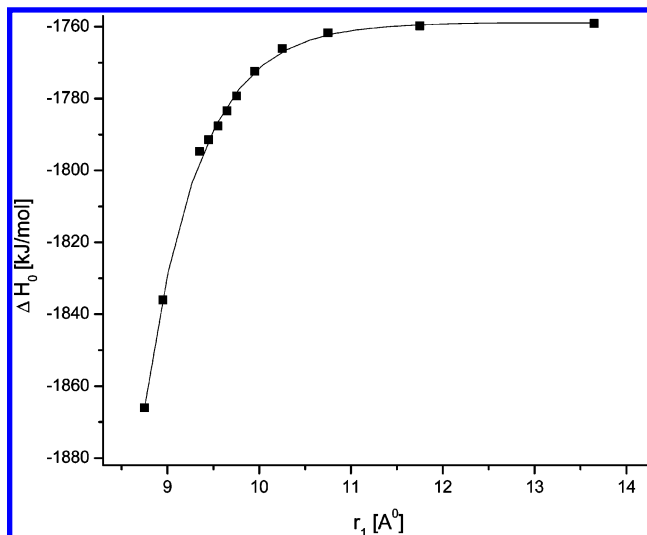


Figure 4. Enthalpy curve for reorganization of the *n*-tetradecanol tetramer (see Figure 1).

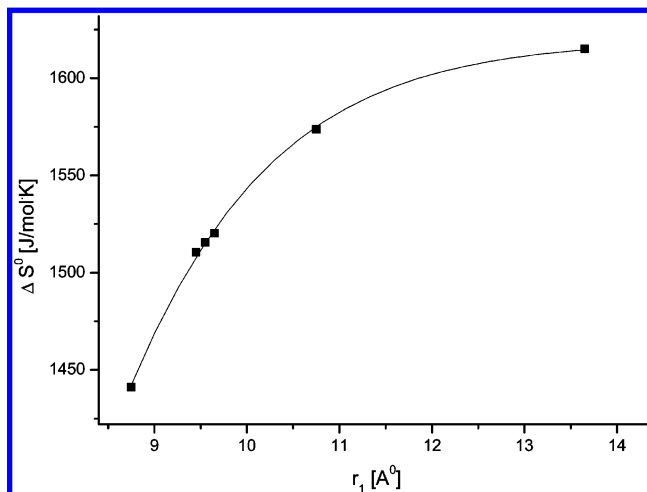


Figure 5. Entropy curve for reorganization of the tetradecanol tetramer (see Figure 1).

entropy value at the nonstationary points at the potential energy (hyper)surface.

It should be noted that a similar situation arises in a number of problems of molecular chemistry, e.g., for reactions with small (or zero) enthalpy barriers, such as recombinations of radicals.¹¹ In these cases, the inflection point at the ΔG (hyper)surface, not at the ΔH (hyper)surface, should be sought. This method is referred to as the variational transition state theory.¹²

Figure 5 illustrates the dependence of the entropy for the cluster shown in Figure 1 on the r_2 value in the points which correspond to the maximum points of the curves shown in Figure 2. These points correspond to a model reaction where the outgoing molecule B is always located in the middle position between dimer A and monomer C. Here the points shown in Figure 5 correspond to the minimum set of imaginary frequencies. When the larger number of imaginary frequencies (4–5) is assumed, then the positions of these points at the plot are lower (because larger number of imaginary vibration modes are excluded from the consideration), whereas the general shape of the dependencies remains the same, only the error becomes somewhat higher. It is seen that with the increase of r_1 the ΔS value becomes higher.

The thermodynamic parameters of the clusterization are defined as the differences between the values of enthalpy,

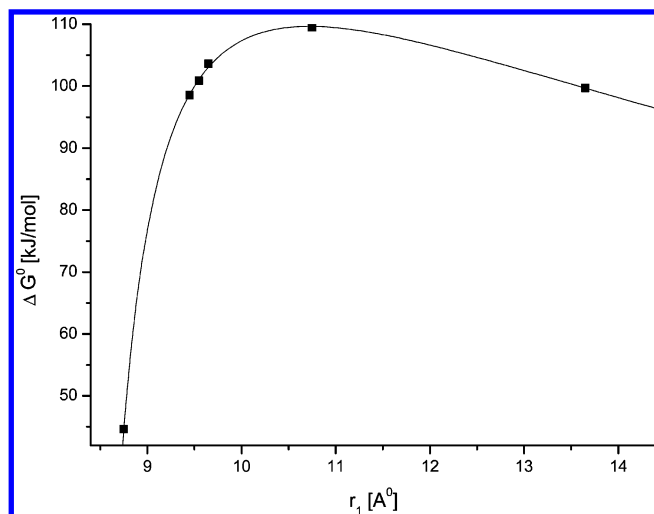


Figure 6. Gibbs energy curve for reorganization of the tetradecanol tetramer (see Figure 1).

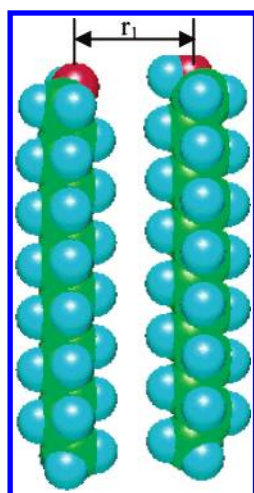


Figure 7. Schematic of dimerization reaction. For the translation motion the reaction coordinate is r_1 .

entropy, and Gibbs energy for the cluster and monomers (subscript mon):

$$\begin{aligned}\Delta H^{\text{cl}} &= \Delta H - m\Delta H_{\text{mon}} & \Delta S^{\text{cl}} &= \Delta S - m\Delta S_{\text{mon}} \\ \Delta G^{\text{cl}} &= \Delta G - m\Delta G_{\text{mon}}\end{aligned}\quad (4)$$

where m is the number of molecules in a cluster. Introducing the ΔH and ΔS values into the expression for the Gibbs energy, and taking into account eq 4, one obtains the dependence of ΔG^{cl} on r_1 shown in Figure 6. The maximum of $\Delta G^{\text{cl}\ddagger} = 110$ kJ/mol observed for $r_1 = 10.5$ Å corresponds to the transition state for the considered recluster model reaction.

If the distance between the trimer and monomer is lower than 10.5 Å, then the formation of the united tetrameric cluster takes place. For higher distances the monomer is detached from the trimer; this detached monomer can then interact with another one, which finally results in the formation of two dimers. It is seen therefore that the entropy factor plays the decisive role in the study of transition states in the recluster reactions for molecular clusters.

Consider next the dimerization of fatty alcohols series to study the effect of the entropy factor on the formation of clusters. For the sake of simplicity, the translation motion of one of the monomers along the dimerization reaction coordinate is as-

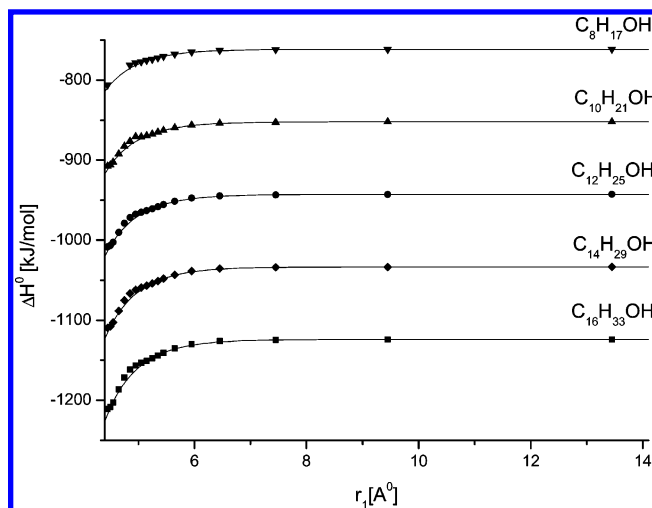


Figure 8. Dependence of dimer enthalpy in the fatty alcohol series on the reaction coordinate r_1 .

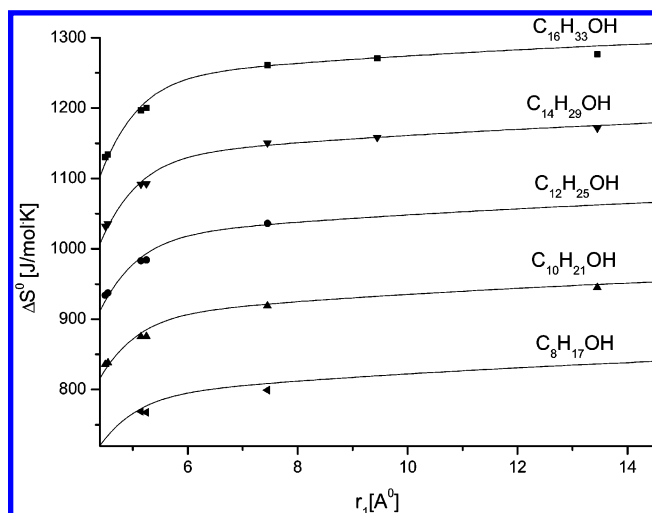


Figure 9. Dependence of dimer entropy in the fatty alcohol series on the reaction coordinate r_1 .

sumed; see Figure 7. In this case, a single reaction coordinate is relevant, which is the distance between the monomer molecules (r_1). Figure 8 illustrates the calculation of the dimer enthalpy for different r_1 values. It is seen that no transition state exists at the potential energy (hyper)surface. The results of the dimers entropy calculations are shown in Figure 9; as before, the points that correspond to the minimum number of imaginary vibration frequencies are shown. As the increase of the ΔH and ΔG values with r_1 is seen to take place, an extremum should exist at the ΔG dependence on r_1 . The Gibbs energies for dimers at 298 K are shown in Figure 10.

For $r_1 \rightarrow 4.45$ Å (which is the average distance between the two monomer molecules in the optimized dimer geometry) the formation of a dimer takes place, whereas for $r_1 \rightarrow \infty$ two monomers are formed that do not interact with each other. For these two limiting cases, the ΔH , ΔS , and ΔG are linearly dependent on the carbon atoms number n .^{8,9} It could be supposed, therefore, that this kind of dependence exists for any distance between the monomers. Therefore, the additive scheme for the description of the transition states in the clustering and recluster reactions of fatty alcohols at the liquid/gas interface could be assumed. In fact, at fixed r_1 values for the enthalpy and entropy of fatty alcohol dimers in the range of $\text{C}_8\text{H}_{17}\text{OH}$ to

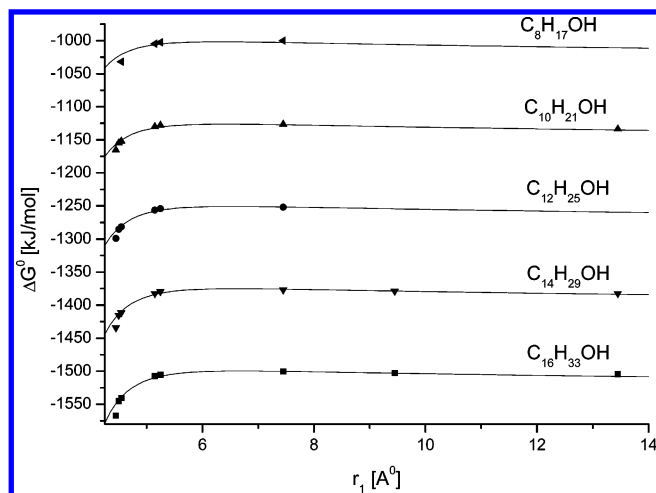


Figure 10. Dependence of the dimer's Gibbs energy in the fatty alcohol series on the reaction coordinate r_1 .

TABLE 1: Parameters of the Correlation Dependences (Eqs 4) for Enthalpy and Entropy of Dimers Corresponding to Various Distances r_1 between Monomer Molecules

r_1	ΔH , kJ/mol			ΔS , J/mol·K		
	$a(r_1)$	$b(r_1)$	S	$c(r_1)$	$d(r_1)$	S
4.5	-401.90	-50.41	0.007	345.13	49.08	0.15
4.55	-401.84	-50.06	0.018	344.82	49.35	0.40
5.15	-400.29	-46.90	0.043	339.78	53.62	1.02
5.25	-400.23	-46.71	0.034	334.87	54.09	0.36
7.45	-399.33	-45.33	0.018	340.02	57.76	3.29
9.45	-399.15	-45.32		369.97	56.31	
13.45	-399.00	-45.31	0.005	392.26	55.41	4.35
monomer	-199.84	-20.71	0.037	211.93	31.96	0.52

TABLE 2: Parameters A , B , and C Used in Model Eq 6 To Calculate the Coefficients $A(r_1)$, $B(r_1)$, $C(r_1)$, and $D(r_1)$ for the Additive Scheme Eq 5

	A	B	C	R	S
$a(r_1)$	-399.13	-2.152	1.273	0.997	0.11
$b(r_1)$	-45.31	-175.93	1.656	0.9998	0.04
$c(r_1)$	424.14	0.394	0.0998	0.97	9.47
$d(r_1)$	56.48	299.25	1.682	0.98	0.87

$C_{16}H_{33}OH$ the dependencies of the types:

$$\Delta H = a(r_1) + b(r_1)n \quad (5a)$$

$$\Delta S = c(r_1) + d(r_1)n \quad (5b)$$

exist, with the coefficients listed in Table 1, where S is the standard deviation. The correlation coefficients R for these dependencies exceed 0.99 and are therefore omitted in the table. The mathematical processing of the data summarized in the Table 1 shows that the $a(r_1)$, $b(r_1)$, $c(r_1)$, and $d(r_1)$ coefficients are well described by the functions:

$$a(r_1) = A/(1 + B \exp(-Cr_1)) \quad (6)$$

and similar relations for $b(r_1)$, $c(r_1)$, and $d(r_1)$. The parameters of the model (6) for the correlation coefficients (5a) and (5b) are listed in Table 2, whereas the results obtained from this model are compared in Figures 8–10 with the data resulting from the direct calculations. It is seen that perfect correspondence exists between the points and curves.

To determine the transition state geometry, one should differentiate the curves shown in Figure 10 with respect to r_1 and set the derivatives to zero. The calculated enthalpies ΔH^\ddagger ,

TABLE 3: Structural and Energetic Parameters for the Dimers in the Transition State of Fatty Alcohols $C_nH_{2n+1}OH$ ($T = 298$ K)

n	$T = 298$ K			
	r_1^\ddagger	ΔH^\ddagger	ΔS^\ddagger	ΔG^\ddagger
8	6.31	-763.69	799.26	-1001.87
10	6.43	-854.39	912.76	-1126.35
12	6.53	-944.97	1026.28	-1250.80
14	6.61	-1035.60	1139.65	-1375.22
16	6.69	-1126.20	1253.10	-1499.63

TABLE 4: Comparison between the Results Obtained in Direct Calculations Using the PM3 Method with the Results Obtained from the Additive Scheme for Thermodynamic Characteristics of Transition States in the Fatty Alcohol Series Dimerization Reaction

N	k_a	$\Delta H^{cl\ddagger}$		$\Delta S^{cl\ddagger}$		$\Delta G^{cl\ddagger}$	
		direct calculation	additive scheme	direct calculation	additive scheme	direct calculation	additive scheme
8	4	-1.13	-1.15	-135.0	-135.8	39.11	39.31
10	5	-1.07	-1.05	-150.3	-150.2	43.71	43.69
12	6	-0.97	-0.95	-165.5	-164.5	48.36	48.06
14	7	-0.87	-0.56	-179.5	-178.9	52.61	52.44
16	8	-0.74	-0.76	-192.2	-193.2	56.53	56.81

entropies ΔS^\ddagger , Gibbs energies ΔG^\ddagger , and intermolecular distances r_1^\ddagger for the dimers in the transition state are listed in Table 3. It is seen that the position of saddle point at the Gibbs energy (hyper)surface depends on the chain length. With the increase of n , the location of the activated complex on the reaction coordinate is displaced toward larger distances; i.e., at larger n values the distance at which the dimer is decomposed into monomers is higher. Therefore, the stability range of the molecular complex becomes wider with the increase of the methylene groups number in the alcohol molecule.

To calculate the energy characteristic of the dimerization, the enthalpy, entropy, and Gibbs energy of two monomers⁸ should be subtracted from the ΔH^\ddagger , ΔS^\ddagger , and ΔG^\ddagger values of the dimers, respectively. The results are listed in Table 4. It is seen that, with the increase of n , the values of dimerization enthalpy in the transition state $\Delta H^{cl\ddagger}$ become lower by absolute value (from -1.13 to -0.74 kJ/mol), whereas the $\Delta S^{cl\ddagger}$ values become higher by absolute value (from -135 to -192 J/mol·K). These small $\Delta H^{cl\ddagger}$ values again indicate the prevailing role of the entropy factor for the existence of the transition state.

The transition states for different alcohols correspond to different r_1 values; however, similarly to the dependencies (5a) and (5b), the linear dependencies of $\Delta H^{cl\ddagger}$, $\Delta S^{cl\ddagger}$, and $\Delta G^{cl\ddagger}$ on n , or on the number of first-type contacts k_a (see 9) can be calculated. These dependencies are

$$r_1^\ddagger = (5.95 \pm 0.03) + (0.094 \pm 0.005)k_a$$

$$n = 5, R = 0.996, S = 0.016 \text{ \AA} \quad (7a)$$

$$\Delta H^{cl\ddagger} = (-1.543 \pm 0.044) + (0.098 \pm 0.007)k_a$$

$$n = 5, R = 0.992, S = 0.023 \text{ kJ/mol} \quad (7b)$$

$$\Delta S^{cl\ddagger} = (-78.4 \pm 2.0) - (14.4 \pm 0.3)k_a$$

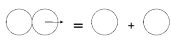
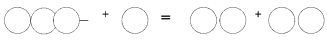
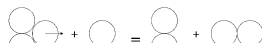
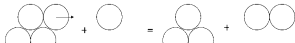

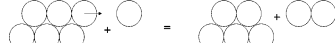
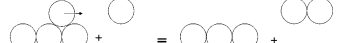


$$n = 5, R = 0.9993, S = 1.00 \text{ J/(mol·K)} \quad (7c)$$

$$\Delta G^{cl\ddagger} = (21.82 \pm 0.55) + (4.37 \pm 0.09)k_a$$

$$n = 5, R = 0.9994, S = 0.28 \text{ kJ/mol} \quad (7d)$$

In Table 4 the calculations made according to the correlations (7a)–(7d) are compared with the results obtained by direct differentiation of the dependencies of ΔG on r_1 . The agreement

TABLE 5: Additive Scheme for the Calculation of Gibbs' Activation Energy (kJ/mol) in the Clusters Reclustering Reactions

n	Reaction	System	k _a	$\Delta G^{\text{cl}\ddagger}$	$\Delta G^{\text{cl}}(\text{reag.})^*$	$\Delta G^{\text{cl}}(\text{prod.})^*$	$\Delta G^{\text{cl}}_{\text{a}}(\text{direct})$	$\Delta G^{\text{cl}}_{\text{a}}(\text{reverse})$
1		C ₈ H ₁₇ OH	4	39.32	8.85	0	30.47	39.32
		C ₁₀ H ₂₁ OH	5	43.69	4.64	0	39.05	43.69
		C ₁₂ H ₂₅ OH	6	48.06	-0.07	0	48.13	48.06
		C ₁₄ H ₂₉ OH	7	52.44	-6.33	0	58.77	52.44
		C ₁₆ H ₃₃ OH	8	56.81	-11.21	0	68.02	56.81
2		C ₈ H ₁₇ OH	12	87.48	25.18	17.69	62.30	69.79
		C ₁₀ H ₂₁ OH	15	92.02	20.40	9.29	71.62	82.74
		C ₁₂ H ₂₅ OH	18	96.06	14.88	-0.14	81.18	96.20
		C ₁₄ H ₂₉ OH	21	98.54	5.57	-12.66	92.98	111.21
		C ₁₆ H ₃₃ OH	24	102.42	0.97	-22.42	101.45	124.83
3		C ₈ H ₁₇ OH	12	126.79	-0.28	17.69	127.07	109.10
		C ₁₀ H ₂₁ OH	15	135.71	-13.67	9.29	149.39	126.43
		C ₁₂ H ₂₅ OH	18	144.12	-27.86	-0.14	171.98	144.26
		C ₁₄ H ₂₉ OH	21	150.98	-41.74	-12.66	192.73	163.65
		C ₁₆ H ₃₃ OH	24	159.23	-57.44	-22.42	216.66	181.65
4		C ₈ H ₁₇ OH	12	117.67	21.11	8.57	96.56	109.10
		C ₁₀ H ₂₁ OH	15	117.40	4.97	-9.03	112.42	126.43
		C ₁₂ H ₂₅ OH	18	116.33	-14.56	-27.93	130.90	144.26
		C ₁₄ H ₂₉ OH	21	115.57	-31.12	-48.08	146.69	163.65
5		C ₈ H ₁₇ OH	16	156.99	6.48	-0.56	150.51	157.54
		C ₁₀ H ₂₁ OH	20	161.09	-21.09	-27.35	182.18	188.43
		C ₁₂ H ₂₅ OH	24	164.40	-51.81	-55.72	216.20	220.12
		C ₁₄ H ₂₉ OH	28	168.01	-80.94	-83.49	248.95	251.50
6		C ₈ H ₁₇ OH	12	153.20	42.82	44.10	110.38	109.10
		C ₁₀ H ₂₁ OH	15	144.58	11.86	18.15	132.72	126.43
		C ₁₂ H ₂₅ OH	18	134.52	-19.59	-9.74	154.11	144.26
7		C ₈ H ₁₇ OH	12	153.20	20.32	44.10	132.88	109.10
		C ₁₀ H ₂₁ OH	15	144.58	-17.36	18.15	161.93	126.43
		C ₁₂ H ₂₅ OH	18	134.52	-53.18	-9.74	187.70	144.26
8		C ₈ H ₁₇ OH	12	153.20	47.20	44.10	106.00	109.10
		C ₁₀ H ₂₁ OH	15	144.58	18.90	18.15	125.67	126.43
		C ₁₂ H ₂₅ OH	18	134.52	-12.66	-9.74	147.18	144.26
9		C ₈ H ₁₇ OH	12	160.77	33.78	51.67	126.99	109.10
		C ₁₀ H ₂₁ OH	15	142.93	-11.69	16.50	154.61	126.43
		C ₁₂ H ₂₅ OH	18	124.60	-32.91	-19.66	157.51	144.26

*Data from ref 8.

is seen to be quite good, which supports the conclusion that the increments determined from eqs 7b–7d can be used in the framework of the additive scheme for the description of the fatty alcohols clustering–reclustering reactions at the interface for arbitrary size of the initial cluster.

In fact, if the numbers of H···H contacts in the transition state between the clusters involved in this transition state, and the numbers of these contacts inside each of these clusters are known, then, using eq 7d and the relations derived in ref 9, one can easily calculate the $\Delta G^{\text{cl}\ddagger}$ value. For the description of the interactions that exist inside the clusters, either the additive scheme described in ref 9 or the direct calculation data could be used. If the $\Delta G^{\text{cl}\ddagger}$ value is calculated using the direct approach, then the free energy of activation for both the direct and reverse reactions can be calculated as

$$\Delta G^{\text{cl}}_{\text{a}}(\text{direct}) = \Delta G^{\text{cl}\ddagger} - \Delta G^{\text{cl}}(\text{reag}) \quad (8a)$$

$$\Delta G^{\text{cl}}_{\text{a}}(\text{reverse}) = \Delta G^{\text{cl}\ddagger} - \Delta G^{\text{cl}}(\text{prod}) \quad (8b)$$

where the free energies of the clustering for products and reagents reported in ref 8 and 9 could be used.

In Table 5 the results obtained from this scheme for the series of fatty alcohols reclustering reactions are summarized; the intercluster interactions in the transition states were described additively, whereas the intracluster interactions were calculated directly. Here the monomers are schematically shown as circles, and the arrows indicate the direction of the translation motion of one (or two) monomers that correspond to the reclustering process. Each scheme shows the initial and resulting cluster structures. The higher the activation energy, the lower the reaction rate; therefore, from the data presented in the table one can estimate how preferential each reaction is as compared to other reclustering processes.^{3,11} It is seen from Table 5 that all the reclustering reactions considered can be subdivided into three types: (i) The reactions in which for all n values the inequality $\Delta G^{\text{cl}}_{\text{a}}(\text{direct}) > \Delta G^{\text{cl}}_{\text{a}}(\text{reverse})$ is correct; i.e., the rate of the direct reaction is lower than the rate of inverse reaction, and therefore the consolidation of clusters takes place. These

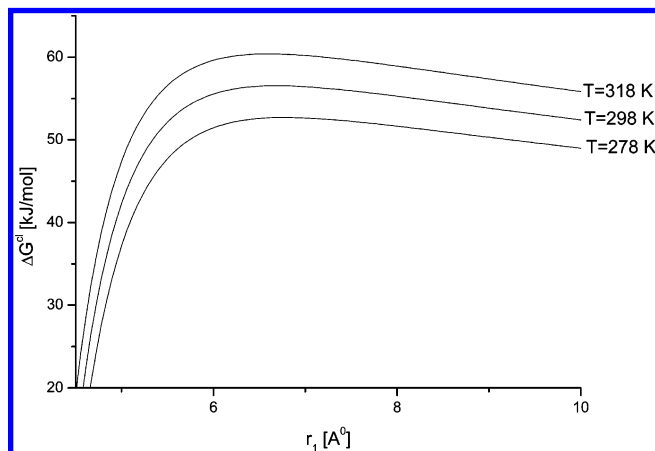
TABLE 6: Temperature Dependence of the Structure and Energetics for the Transition States of Fatty Alcohols Dimerization Reactions

<i>n</i>	<i>T</i> = 278 K				<i>T</i> = 298 K				<i>T</i> = 318 K			
	<i>r</i> ₁ [‡]	Δ <i>H</i> ^{cl‡}	Δ <i>S</i> ^{cl‡}	Δ <i>G</i> ^{cl‡}	<i>r</i> ₁ [‡]	Δ <i>H</i> ^{cl‡}	Δ <i>S</i> ^{cl‡}	Δ <i>G</i> ^{cl‡}	<i>r</i> ₁ [‡]	Δ <i>H</i> ^{cl‡}	Δ <i>S</i> ^{cl‡}	Δ <i>G</i> ^{cl‡}
8	1.94	−0.90	−134.3	36.42	1.86	−1.13	−135.0	39.11	1.78	−1.46	−136.1	41.83
10	2.06	−0.81	−149.4	40.72	1.98	−1.07	−150.3	43.71	1.89	−1.41	−151.4	46.73
12	2.16	−0.70	−164.6	45.06	2.08	−0.97	−165.5	48.36	1.99	−1.30	−166.6	51.68
14	2.25	−0.57	−178.4	49.03	2.16	−0.87	−179.5	52.61	2.07	−1.21	−180.6	56.21
16	2.32	−0.48	−191.3	52.70	2.24	−0.74	−192.2	56.53	2.15	−1.08	−193.3	60.39

are reactions 3, 6, 7, and 9. (ii) The reactions in which for all *n* values the inequality $\Delta G_a^{\text{cl}}(\text{direct}) < \Delta G_a^{\text{cl}}(\text{reverse})$ is correct; i.e., the rate of the direct reaction is higher than the rate of inverse reaction, and therefore the decrease of cluster sizes should take place. These are the reactions 2, 4, and 5. (iii) The reactions in which for small *n* values the disaggregation of clusters should be observed, whereas for larger *n* values (*n* > 12) the aggregation takes place. It should be noted that, from the kinetic point of view, the transformation of two dimers into trimer and monomer is more probable for the formation of the triangular trimer, and less probable if the linear trimer is formed; this fact is in agreement with the data of our previous studies⁹ indicating that the triangular trimer is more stable than the linear one.

The procedure described above can be used to describe the transition states of clustering and recluster in large (and also infinite) clusters. Consider the processes of the attachment of a monomer to the infinite linear or infinite star cluster, and the recluster of the infinite linear into the infinite star cluster. The relations derived in ref 9 for the Gibbs energy of linear and star cluster are $\Delta G^{\text{cl}}_1 = [18.08 - 3.71(n/2)]m_1$ and $\Delta G^{\text{cl}}_2 = [34.70 - 3.71n]m_2$, respectively, where *m*₁ is the number of monomers in the linear cluster, and *m*₂ is the number of monomers in the star cluster (*m*₁ and *m*₂ should be large enough). Using these relations and eq 7d, one can calculate the $\Delta G^{\text{cl}‡}$ value, and then from eqs 8a and 8b the Gibbs activation energies for the direct and reverse reactions can be calculated. Thus, for the attachment of a monomer to the linear infinite cluster one obtains $\Delta G_a^{\text{cl}}(\text{direct}) = 21.82 + 2.19n$ and $\Delta G_a^{\text{cl}}(\text{reverse}) = 3.74 + 4.04n$, and for the attachment of a monomer to the infinite star cluster one obtains $\Delta G_a^{\text{cl}}(\text{direct}) = 43.64 + 4.37n$ and $\Delta G_a^{\text{cl}}(\text{reverse}) = 8.94 + 8.08n$. It can be easily shown from these dependencies that in both cases the rate of the direct reaction is larger than the rate of reverse reaction for *n* ≥ 10, which corresponds to the aggregation of clusters. Comparing the activation energies of direct reactions for these processes one can see that the $\Delta G_a^{\text{cl}}(\text{direct})$ value for the first reaction is lower than that for the second reaction at any *n* value; i.e., from the kinetic point of view the formation of linear clusters is preferential as compared with the formation of star clusters, whereas from the thermodynamic point of view for *n* ≥ 10 the reverse process is favorable. Using the procedure described above, for the transfer of a single monomer from the infinite linear cluster to the infinite star cluster one obtains $\Delta G_a^{\text{cl}}(\text{direct}) = 47.38 + 8.41n$ and $\Delta G_a^{\text{cl}}(\text{reverse}) = 30.76 + 10.27n$. It is seen that for *n* ≥ 9 the rate of the direct reaction is higher than the rate of the reverse reaction; i.e., the transformation of the linear cluster into the star cluster should prevail (this process is more probable from the kinetic point of view and is more preferential from the thermodynamic considerations. Note that the formulas above are applicable not only to the transfer of a single monomer from the linear cluster to the star one but also to the attachment of any linear cluster.

The theoretical results presented above can possibly explain the preferential initial formation of “snowflake”-like clusters

**Figure 11.** Dependence of Gibbs' energy for the hexadecanol dimerization reaction on the reaction coordinate and temperature.

when the clustering of liquid alcohols at the interface takes place; cf. Figure 6 in ref 9: the linear clusters, which are more possible to be formed from the kinetic point of view, are attached to the star nucleus; thus the snowflake-like particle is formed, to which the monomers and other clusters are then attached.

Finally, the dependence of the activated complex dimerization reaction parameters on the temperature can be analyzed. It can be seen from the results obtained from direct calculations that in the considered temperature range 278–328 K the $\Delta H^{\text{cl}}(r_1)$ and $\Delta S^{\text{cl}}(r_1)$ values are almost independent of the temperature, and the temperature dependence of $\Delta G^{\text{cl}}(r_1)$ is determined by eq 2. Differentiating the dependence of $\Delta G^{\text{cl}}(r_1)$ with respect to *r*₁ and setting the derivative to zero, one can analyze the structure and energetic parameters of transition states. The results of the calculations are presented in Table 6, and the dependence of ΔG^{cl} on *r*₁ for the hexadecanol dimerization reaction at various temperatures is shown in Figure 11. It is seen that in the dimerization reaction transition state, with the temperature increase the distance between the monomers decreases, and the activation barrier becomes higher. Therefore, in the dimer formation regime (on the contrary to the cluster formation regime) a weak dependence of surface pressure on the monolayer compression rate should exist (because the $\Delta G^{\text{cl}‡}$ value for the dimerization is small), and even more weak dependence of the pressure jump on the temperature. These guesses are in agreement with the experimental data reported in ref 15.

Figure 12 illustrates the surface pressure isotherms of tetradecanol monolayers at 25 °C, measured at different rates of the monolayer compression. The experimental method used has been described in refs 8 and 9. It is seen that the higher the compression rate of the monolayer, the higher the surface pressure value that corresponds to the onset of condensation (a 10-fold increase of the compression rate results in a pressure increase from 0.3 to 1.0 mN/m. This fact shows that the monolayer is oversaturated by monomers or small aggregates¹⁵ and indicates that a kinetic barrier exists for the clustering in the tetradecanol monolayer. At the same time, this barrier is

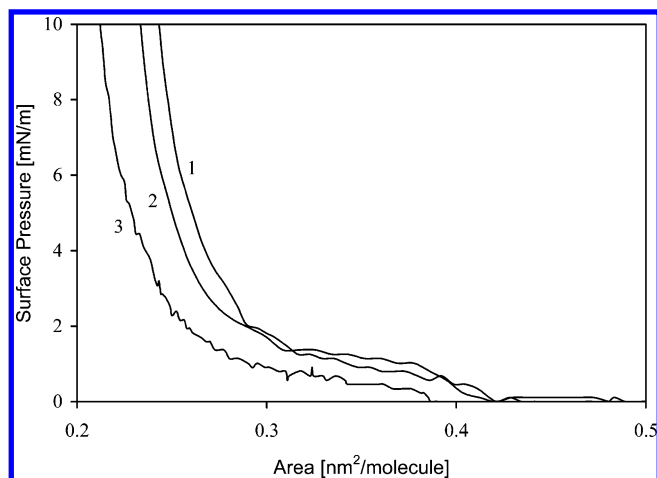


Figure 12. Dynamic surface tension for the compressed monolayers of *n*-tetradecanol at 25 °C and $dA/dt = 1 \text{ nm}^2/\text{min}$ (curve 1), $0.5 \text{ nm}^2/\text{min}$ (curve 2), and $0.1 \text{ nm}^2/\text{min}$ (curve 3).

quite low, because the dynamic pressure jump is much smaller than the barrier which exists, for example, in the palmitoyl-D-allo-threonin methyl ester monolayers.¹⁵ This result seems to be in agreement with the fact that for the palmitoyl-D-allo-threonin methyl ester not only the activation energy for clustering is much higher than the corresponding value for tetradecanol but also the enthalpy constituent of this energy is quite significant. The results obtained at the temperature of 30 °C are rather similar to those presented in Figure 12; this fact is in agreement with the theoretical conclusions which indicate that the activation barrier of the tetradecanol clustering is mainly entropy-related.

Conclusions

The quantum chemical PM3 approximation provides reasonable values for the thermodynamic characteristics of the transition states for the formation of alcohol dimers with various structures at the air/water interface. It is shown that at the potential energy (hyper)surface of the reactions studied, the saddle point that corresponds to the transition states does not exist, in contrast to the Gibbs energy (hyper)surface. This fact indicates that the entropy factor plays a crucial role with regard to the existence of transition states in the reactions of clustering and reorganization of fatty alcohols $C_nH_{2n+1}OH$ at the air/water interface. The dependencies of the calculated values of enthalpy, entropy, and Gibbs energy on the reaction coordinate were approximated by analytical expressions, and from the differentiation of these expressions, geometry and energetics of the transition states were determined. In particular, it was shown that the position of the saddle point at the Gibbs energy surface depends on the alkyl chain length. With the increase of n , the position of the activated complex at the reaction coordinate

corresponds to larger distances, which indicates that the increase of the number of methylene groups in the alcohol molecule leads to an extension of the stability range of the molecular complex. It is shown that in the points corresponding to the transition states, similarly to the points in which the potential energy is minimal, the calculated values of enthalpy, entropy, and Gibbs energy for the cluster formation and reorganization can be satisfactorily represented by a linear dependence on the number of CH_2 groups in the alcohol molecule. On this fact, the additive scheme could be based, which describes the transition states in the clustering and reclusterings reactions of fatty alcohols, including large and infinitely large clusters. The validity of the additive model is illustrated using as example the transition states of a series of clustering and reclusterings reactions in fatty alcohol monolayers. It was shown that, whereas from kinetic considerations the formation of linear clusters is more probable than the formation of star clusters, the process of the attachment of any linear cluster to a star cluster is more probable from kinetic considerations and is more advantageous from the thermodynamic standpoint. With the increase of temperature, the distance between the monomers in the transition state of the dimerization becomes smaller, and also the activation barrier becomes higher as the temperature increases.

This approach can be applied for studies of clustering and reclusterings in other systems. In future, a more accurate scheme for the entropy calculation in the nonstationary points at the potential energy (hyper)surface should be realized corroborated by corresponding experimental studies.

References and Notes

- (1) Benson, S. W. *Foundations of Chemical Thermodynamics*; McGraw-Hill: New York, 1960.
- (2) Bamford, C. H.; Tipper, C. F. H., Eds. *Comprehensive Chemical Kinetics*; Elsevier: Amsterdam, 1969–1980; 22 vols.
- (3) Neil, S. I. *Physical Organic Chemistry*; Longman Scientific & Technical: Singapore, 1995.
- (4) Hehre, W. J.; Radom, L.; Scheyer, P. von R.; Pople, J. A. *Ab Initio Molecular Orbital Theory*; John Wiley & Sons: New York, 1986.
- (5) Baker, J. J. *Comput. Chem.* **1986**, 7, 385.
- (6) Peng, C.; Schlegel, H. B. *Isr. J. Chem.*, **1993**, 33, 449.
- (7) Rusanov, A. I.; Kuni, F. M.; Shchekin, A. K. *Colloids Surf. A* **1997**, 128, 13; Rusanov, A. I. *Fizicheskie Ravnovesiya i Poverkhnostnye Yavleniya*; Khimija: Leningrad, 1967.
- (8) Vysotsky, Yu. B.; Bryantsev, V. S.; Fainerman, V. B.; Vollhardt, D.; Miller, R. J. *Phys. Chem. B* **2002**, 106, 121.
- (9) Vysotsky, Yu. B.; Bryantsev, V. S.; Fainerman, V. B.; Vollhardt, D. *J. Phys. Chem. B* **2002**, 106, 11285.
- (10) Stewart, J. J. P. *MOPAC 2000.00 Manual*; Fujitsu Ltd.: Tokyo, Japan, 1999. Stewart, J. J. P. *J. Comput. Chem.* **1989**, 10, 209.
- (11) Jensen, F. *Introduction to Computational Chemistry*; John Wiley & Sons: Chichester, U.K., 1999.
- (12) Truhlar, D. G.; Gordon, M. S. *Science* **1990**, 249, 491.
- (13) Hobza, P.; Zahradnic, R. *Intermolecular Complexes. The Role of van der Waals System in Physical Chemistry and in the Biodisciplines*; Academia Praga, Prague, 1988.
- (14) Scheiner, S., Ed. *Molecular Interactions. From van der Waals to Strongly Bound Complexes*; John Wiley & Sons: Chichester, U.K., 1997.
- (15) Vollhardt, D.; Fainerman, V. B. *J. Phys. Chem. B* **2002**, 106, 345–351.